

5.3 Mineralogical Composition

The mineralogy of the dunes and sand sheets is analyzed by the method described in Sect. 4.5.1. The output of this method is images in which the absorption depths corresponding to the minerals of interest are stored in different channels. By superimposing these absorption depth images onto the original OMEGA images, mineral absorption depth on the surface can be mapped (see Fig. 27). For the individual locations, at least two different OMEGA orbits (where available) were used to verify the results. Comparing images from several orbits improves the chances of detecting and eliminating the residual influence of surface or atmospheric dust which might mask the mineralogical signature by a featureless spectrum declining to higher wavelengths ('blue slope'). Atmospheric dust varies over time; thus, these spectral influences should have changed by the time of the next observation (cf. Sect. 5.3.1). Surface dust coatings may disappear in the meantime. If a blue slope is obvious in one observation and gone in the second, the conclusion is that the first observation was contaminated by dust and cannot be used for mineral detection. Correlating mineral spectra for both orbits provide the best verification.

In addition to the mineral maps obtained by the ratio technique adapted from *Poulet et al.* (2007), the individual spectra of every dune deposit were analyzed as well. This is very important in order to avoid misinterpretations (see Sect. 5.3.1). To enhance the spectral signature of the dark material, spectral ratios are generated by dividing the I/F of atmospherically corrected spectrum of the dark material by a reference spectrum. The latter was obtained on the same OMEGA orbit (same atmospheric path length and instrumental effects) from a nearby dusty region exhibiting no mafic mineral features. Thus, residual atmospheric and instrumental effects were cancelled out, leaving the spectral properties of the material of interest in the ratio spectrum [*Mustard et al.*, 2005].

A typical OMEGA I/F reflectance spectrum of dark material is shown in Fig. 41a, black curve. Fig. 41b shows the same spectrum compared to a reference spectrum obtained on the same orbit, the ratio of both, and a laboratory spectrum of olivine. While the original spectrum in Fig. 41a implies pyroxene abundance, the ratio spectrum in Fig. 41b emphasizes the broad 1- μm olivine band compared to the laboratory spectrum. The discrepancies between the olivine laboratory spectrum and the ratio spectrum are caused by differences in the spectral resolution of the laboratory and OMEGA spectrometers. However, the position and shape of the absorption band correlates. Thus, the ratio helps to identify that the dark material spectrum contains spectral signatures comparable to a mixture of olivine and pyroxene at this locality. This mineral mixture has a spectral signature which not only exhibits the two absorption bands at 1 μm and 2 μm that are typical of pyroxene but also features a characteristic shape of the 1- μm band, which is broad and gently inclined to 1.5 μm due to the presence of olivine (see green and red spectra in Fig. 41b).

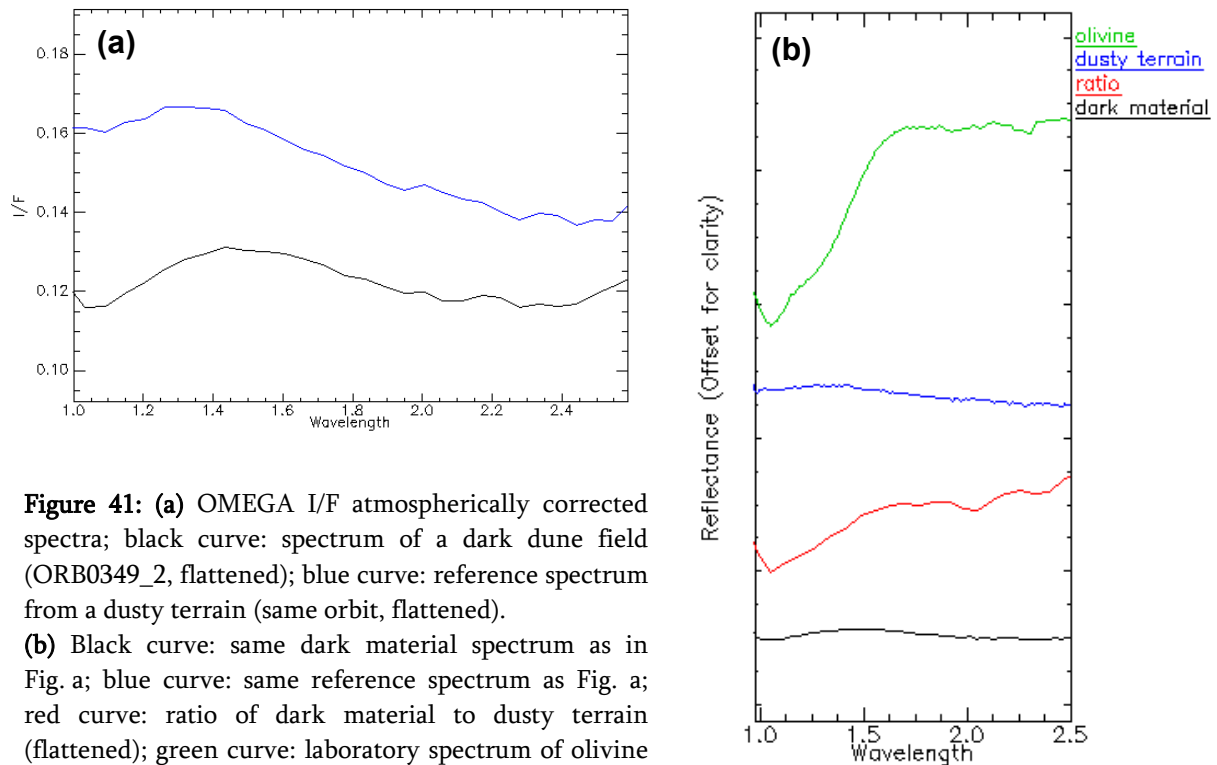


Figure 41: (a) OMEGA I/F atmospherically corrected spectra; black curve: spectrum of a dark dune field (ORB0349_2, flattened); blue curve: reference spectrum from a dusty terrain (same orbit, flattened). (b) Black curve: same dark material spectrum as in Fig. a; blue curve: same reference spectrum as Fig. a; red curve: ratio of dark material to dusty terrain (flattened); green curve: laboratory spectrum of olivine (see text for discussion).

5.3.1 Uncertainties

Several factors might lead to misinterpretations of the mapping results. As already mentioned in Sect. 4.5.1, the presence of water ice and CO₂ ice can influence the detection of hydrated minerals. Both ices have an absorption band centred at 2 μm that may affect the detection of hydrated minerals whose diagnostic absorption bands are centred at 1.9 μm. Mafic mineral detection can be influenced by the presence of ice [Poulet *et al.*, 2007] because the characteristic H₂O ice absorption at 1.5 μm and the CO₂ absorption at 1.43 μm lie within the spectral range that is characteristic for pyroxene and olivine. Therefore, pixels showing ice absorptions are disregarded in the determination of dark material mineralogical composition. However, the detection of ice is meaningful because it can act as a cementing agent on dune surfaces. Thus, this information was regarded in the determination of indurated dunes (see Sect. 5.7). Fine-grained coatings on the surface might mask the spectral signature of a material in the visible and near-infrared wavelength range [Singer and Roush, 1983; Christensen *et al.*, 1998]. Due to the increasing transparency of surface coatings at longer wavelengths, this effect is less important in the near-infrared than in the visible spectral range, so that pyroxene and olivine can be detected despite the presence of a surface coating [Poulet *et al.*, 2007]. Poulet *et al.* (2007) even interpreted the resulting blue slope of the spectrum as an indirect detection of basaltic materials such as pyroxene and olivine. However, due to the

uncertainty inherent in this interpretation, spectral ratios were computed in this work to discover a possible mafic signature. Dark materials exhibiting a strong blue slope spectrum and lacking an indication of mafic composition in the spectral ratio are interpreted as dust-covered (labelled as 'no mafics' in Fig. 50). The influence of aerosols (atmospheric dust) has a comparable blue slope expression in the spectral shape. However, this effect is highly variable with time. Thus, the analysis of multiple OMEGA observations acquired at different times, and the comparison of the different results, permitted verifying temporal variations and selecting unaffected observations. Furthermore, the influence of atmospheric dust is strongest in the visible wavelength range and decreases with increasing wavelength due to the growing transparency of aerosols [*Singer and Roush, 1983*]. This small influence allows neglecting atmospheric variations in mineral detection in the near-infrared range. The grain size distribution as well as mineral mixtures has a strong influence on the absorption band depth. Especially the discrimination between forsterite and fayalite is critical with varying grain size because of the strong influence on the 1 μm -band [*Poulet et al., 2007*]. *Poulet and Erard (2004)* and *Poulet et al. (2007)* present detailed simulations applied to test the influence of mineral mixtures and grain sizes on the spectral shape of minerals. In addition to other factors, increasing grain sizes result in decreasing depths of olivine absorption, making it difficult to discriminate between coarse-grained forsterite and fine-grained fayalite, for example. However, for this analysis it was not diagnostic to discriminate between the olivine types. Thus, the forsterite and fayalite criteria were merged into one group for olivine detection.

5.3.2 Results and Discussion

A careful spectral analysis was made of every location, including mineral mapping and an analysis of the spectra and ratios to substantiate the mapping results. The OMEGA orbits used for the respective localities are listed in Appendix. By way of example, Fig. 42 shows the mapping result for the Dawes Crater located in Terra Sabea (9.2°S, 38°E). The left-hand image shows the distribution and band depth of the 2- μm feature corresponding to the occurrence of pyroxene. The right-hand image shows the depth of the 1- μm olivine absorption band (see Sect. 4.5.1). The band depths are colour-coded and the absolute values can be read in the legend. The variation of band depth depends on the relative abundance and grain size of the minerals [*Poulet et al., 2005*]. In Dawes Crater as well as in many other localities, pyroxene is the dominant mineral. The strongest pyroxene absorption is mapped in areas where the dark material builds dunes. The surrounding sand sheets exhibit shallower pyroxene bands. Olivine minerals occur solely in the dune areas and not in the surrounding thin wind-blown sand sheets. The analysis of the spectra confirms the mapping results. The ratio of the dark dune spectrum to the reference spectrum emphasizes the broad 1- μm olivine absorption band (see Fig. 42c). Furthermore, the deep 2- μm pyroxene band is clearly visible in the ratio spectrum. If pyroxene alone were involved, the 1- μm absorption band would be much narrower and incline faster. The

spectra confirm the mapping results, which imply that the dark dunes in Dawes Crater have a mineralogical composition of pyroxene and olivine.

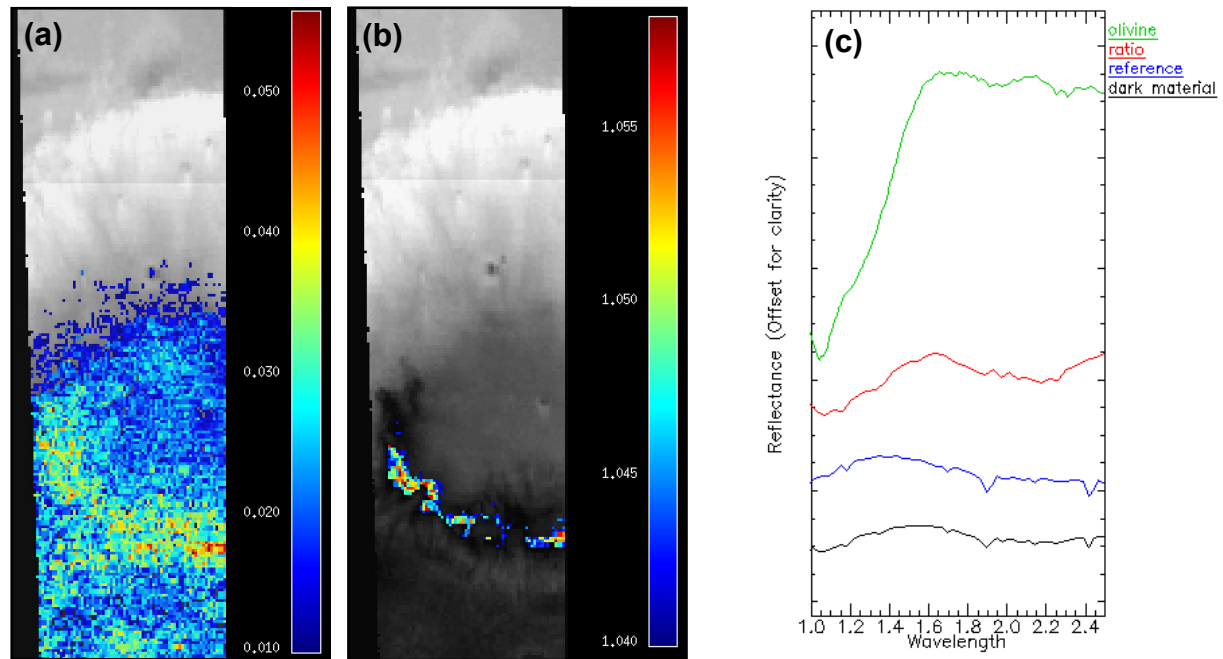


Figure 42: Results of the OMEGA spectral analysis of dark material in Dawes Crater (Terra Sabea, 9.2°S, 38°E; ORB2384_4).

(a) Mapping of pyroxene inferred from the depth of the 2- μ m band. (b) Mapping of olivine inferred from the 1- μ m band. (c) OMEGA ratio spectrum (red) of dark material (black) to reference spectrum (blue) compared to laboratory spectrum of olivine (green).

A similar result was obtained for Trouvelot Crater, located in Oxia Palus (16.3°N, 346.5°E, western Arabia Terra). Pyroxene is the dominant mineral, while olivine solely occurs in the dark patch in the smaller crater superimposed onto Trouvelot's crater floor. The band depth of olivine in that area is very shallow. However, the spectral ratio confirms the detection of olivine in Trouvelot Crater. At the eastern margin of that intra-crater patch there is a small area showing a strong absorption feature at 1.9 μ m corresponding to hydrated minerals (Fig.43c and 43e). The occurrence of hydrated minerals in Meridiani Planum and nearby terrains has been reported before by several authors [e.g. *Gendrin*, 2005; *Poulet et al.*, 2008; *Christensen et al.*, 2004b]. A complex of light-toned layered outcrops [*Edgett*, 2002] can be found further to the south-east on Trouvelot's crater floor, bearing a striking resemblance to the so-called Interior Layered Deposits (ILDs). Many authors analyzed such deposits in Valles Marineris and the Chaotic Terrains on Mars [e.g. [*Nedell et al.*, 1987; *Fuerten et al.*, 2005; *Chapman et al.*, 2007; *Sowe et al.*, 2007]. Different kinds of sulphates were found on the flanks of the ILDs [*Hauber et al.*, 2006; *Roach et al.*, 2007]. These hydrated minerals point to an aquatic genesis of the layered deposits [*Gendrin*, 2005]. If this hypothesis is right, it could be likely that the complex of light-toned layered outcrops at Trouvelot Crater is of similar origin. Thus, if the dark material had emerged already at that time, these aquatic processes could be the cause of the hydration of the dark material in this locality as well.

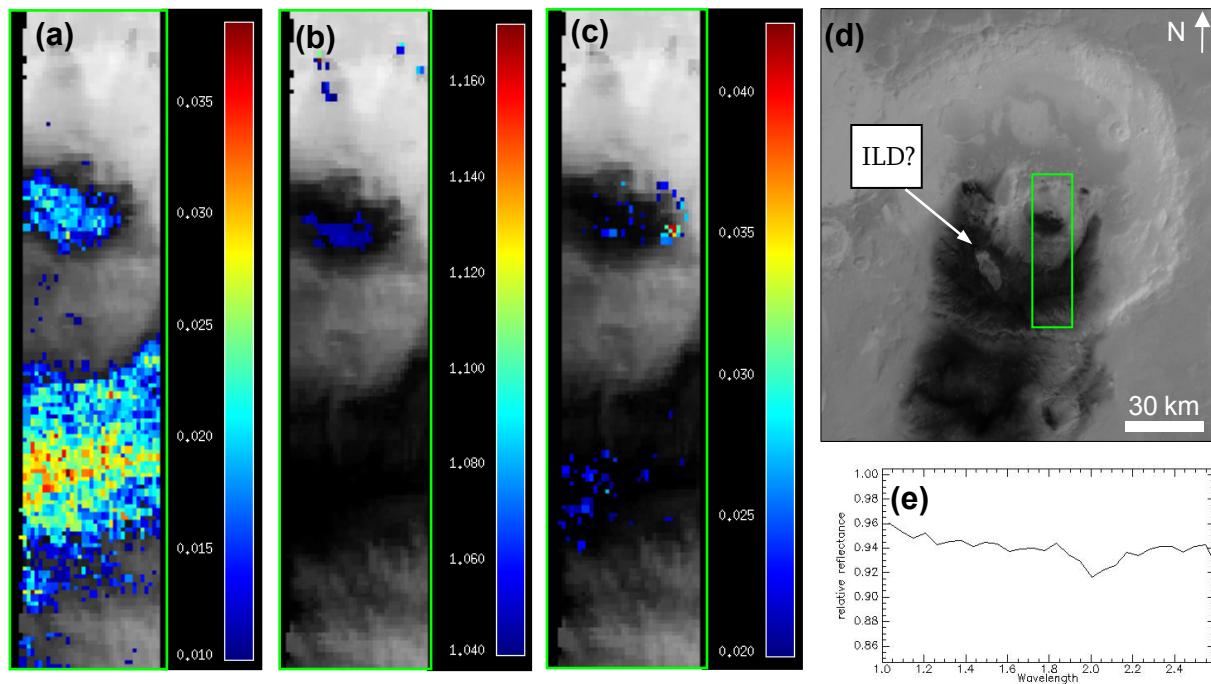


Figure 43: Results of the OMEGA spectral analysis of dark material in Trouvelot Crater (western Arabia Terra, 16.3°N, 346.5°E; ORB1260_2).

(a) Mapping of pyroxene inferred from the depth of the 2- μ m band. (b) Mapping of olivine inferred from the 1- μ m band. (c) Mapping of hydrated minerals inferred from the depth of the 1.9- μ m band. (d) Context image of Trouvelot Crater showing footprint of OMEGA subset in Fig. a, b and c (HRSC mosaic of 3268_0000 and 3275_0000). (e) OMEGA spectrum of hydrated minerals showing the absorption band near 1.9 μ m detected at the eastern margin of the dark patch within the smaller crater inside Trouvelot Crater.

However, one might ask why not the entire dark material was affected by this hydration because a lacustrine environment would span the whole crater floor. In addition to Trouvelot Crater, hydrated minerals were detected in a crater near Mamers Valles (Fig. 44) and in some craters in Meridiani Planum (cf. Fig. 50). The occurrence of hydrated minerals in western Arabia Terra was previously reported by several authors [e.g. *Arvidson et al.*, 2005; *Gendrin*, 2005; *Poulet et al.*, 2005; *Jouglet et al.*, 2007; *Loizeau et al.*, 2007a; *Poulet et al.*, 2008]. *Loizeau et al.* (2007) found large bright outcrops comprising phyllosilicates near Mawrth Vallis. One hypothesis says that the formation of these phyllosilicate-rich units could be caused by the alteration of volcanic ash deposits [*Loizeau et al.*, 2007a]. These findings support the local alteration hypothesis of the dark material in Trouvelot Crater. *Poulet et al.* (2008) also found hydrated minerals co-located with mafic materials in craters in Meridiani Planum and western Arabia Terra. Hydrated materials cover large segments of the etched terrain in Meridiani Planum (unit E at *Poulet et al.* (2008)). *Poulet et al.* (2008) reported that the dark pyroxene-bearing dunes overlay this brighter etched terrain in their research areas. This being so, they suppose that the spectra of the OMEGA pixels of these localities represent a mixture of pyroxene-bearing dune material and the hydrated materials of the etched terrain. This scenario probably also applies to the craters in Meridiani Planum where hydrated minerals are reported in this work, because they are located very close to the craters analyzed by *Poulet et al.*

(2008). Unfortunately, the lack of high-resolution image data for these craters makes it impossible to prove this theory. In the case of Trouvelot Crater (Fig. 43), further analyses will have to show whether the hydration spectral signature is associated with the dark material itself, caused by hydrated material underneath the dunes, or shining through a thin dark sand sheet. This can be done as soon as high-resolution image data become available for this locality.

The site of hydrated mineral detection near Mamers Valles (34.0°N, 17.0°E) is located on a crater floor in Ismenius Lacus. *Poulet et al.* (2005) assumed these hydrated minerals to be Fe- and Mg-bearing phyllosilicates. The crater shows obvious morphological indications of glacial processes in the form of fan-shaped glacial features and glacial troughs [*Di Achille and Ori, 2008*]. Dated to the Amazonian epoch by *Di Achille et al.* (2008), these glacial processes might have caused an aquatic alteration of the crater floor material. As shown in Fig. 44, there is a lobate feature emanating from the south-east towards the dark material patch at the crater centre. *Di Achille et al.* (2008) suppose that it was formed as a glacial lacustrine ice-contact delta. The direct contact between this lobate feature representing the remnants of the former glacier and the dark material patch could be the reason for a local alteration of dark material when melt water caused the hydration of minerals in the contact zone (Fig. 45, case Ia and Ib). This scenario presupposes that active glacial processes and the dark material co-existed in this crater. If this is the case, it is an indicator for the alteration and formation of phyllosilicates during the Amazonian epoch. Even today, the coexistence of ice and dark material can be observed in a crater in Vastitas Borealis, which exhibits a water ice cap covering a dark material deposit in the crater centre (Fig. 47). Although this recent example is from a crater located in higher latitudes (70.5°N) supporting the stability of ice, the distinct glacial features dated to the Amazonian in the crater near Mamers Valles close to 30° northern latitude suggest that ice and dark material might coexist at the present time. A second scenario suggests a small melt water pond or puddle between the dark patch and the glacier (Fig 45, case II). Material from the dark patch nearby might have accumulated in a thin sheet in this pond, resulting in local lacustrine material alteration. This hypothesis is underpinned by the profile of the crater floor, which features a depression in the place where the hydrated minerals were detected (Fig. 46a). Regarding the chronology of ice and material deposition, this hypothesis does not presuppose the presence of dark material when glacial processes were active. Yet the material must have been deposited before the small pond disappeared. It may be assumed, however, that the water in the pond did not remain stable for long after the retreat of the ice because the low air pressure did not support liquid water in Amazonian times. However, high-resolution CRISM image data reveal that the dark material is very thin at this location, so that an alternative explanation is called for. The hydration signal detected from OMEGA data might originate from hydrated material underneath the dark material. In this third scenario, glacial lacustrine processes caused a hydration of the crater floor material, as mentioned above. Thus, the retreat of the glacier might have caused the exposure the formerly covered phyllosilicates (Fig. 45, case III). The hydrated crater floor material was subsequently covered by a thin

sheet of dark material deposited afterwards, which is the situation today. However, if this is the case, the question is why the spectral signal of hydration was only found on the margin of dark patch itself (Fig 44b) and not on the surrounding crater floor. A local erosion of hydrated material in the surrounding could be the reason for that situation. Chronologically, this scenario does not require a co-existence of dark material and ice. The dark material might have been deposited after the decrease of the glacial activity later in the Amazonian epoch.

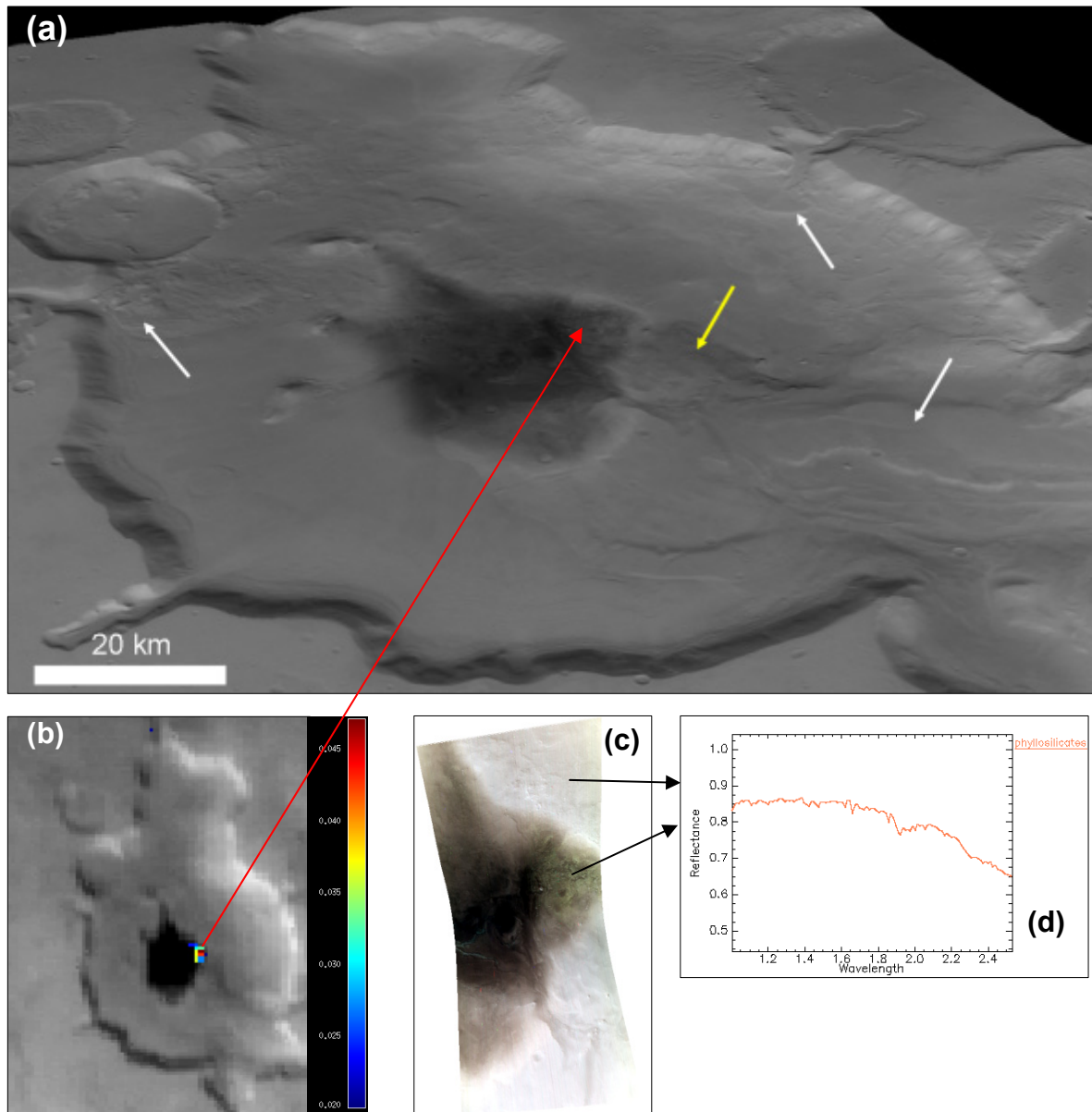


Figure 44: Glacial features and hydrated minerals in a crater in Ismenius Lacus, near Mamers Valles (34.0°N, 17.0°E).

(a) HRSC perspective view from orbit 2192_0009. White arrows indicate fan-shaped glacial features emanating from glacial troughs. The yellow arrow marks the lobate feature that extends to the dark deposit in the crater centre. (b) Mapping of hydrated minerals inferred from the 1.9- μm band in OMEGA orbit ORB1296_6. (c) CRISM observation HRL0000853D, colour composite of bands 13 (1.08 μm), 87 (1.5 μm) and 233 (2.5 μm). The high spatial resolution of 19 cm/pixel reveals the thinness of the sand sheet. (d) CRISM spectral ratio of dark patch to crater floor (see black arrows) enhancing the spectral features of the hydrated material (1.9- μm absorption band) detected at the right-hand margin of the dark patch. (see text for discussion)

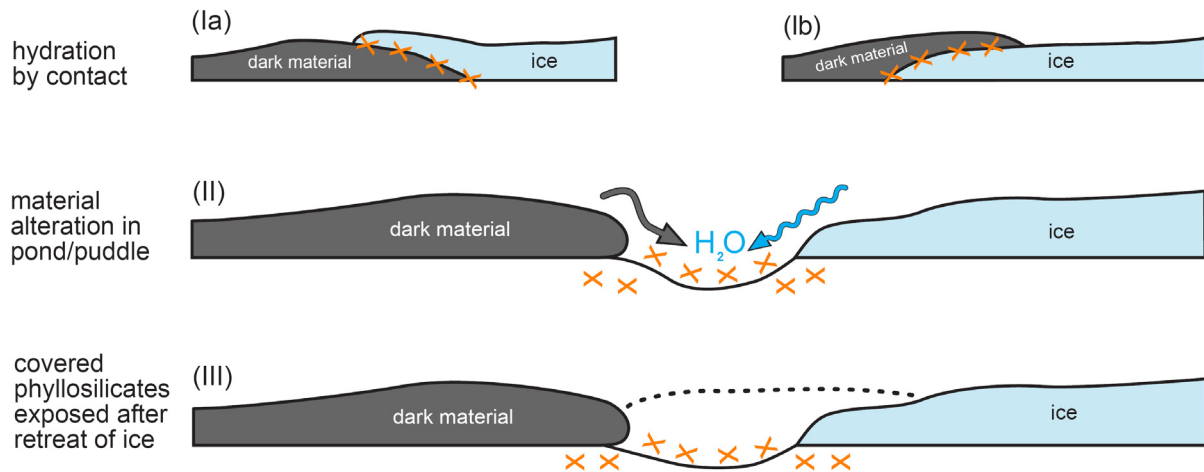


Figure 45: Different scenarios for hydration caused by glacial processes in the crater shown in Fig. 44.

(I) Hydration of dark material caused by direct contact with ice which might have covered the dark material (Ia) (for an analogue see Fig. 47) or vice versa (Ib). **(II)** Hydration of a small proportion of dark material accumulated in a melt water-filled pond or puddle in between the ice and the dark deposit. **(III)** Exposure of phyllosilicates (hydrated crater floor material) after the retreat of the ice. Dark material has not been altered in this case. (see text above for discussion)

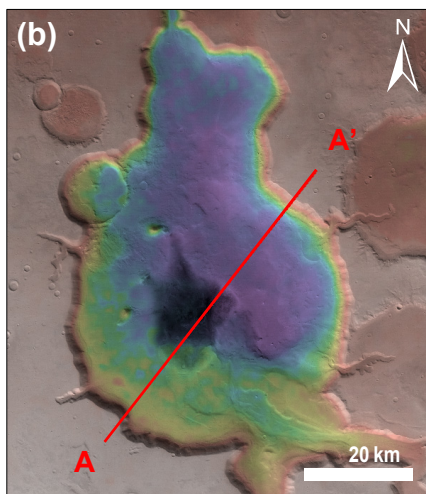
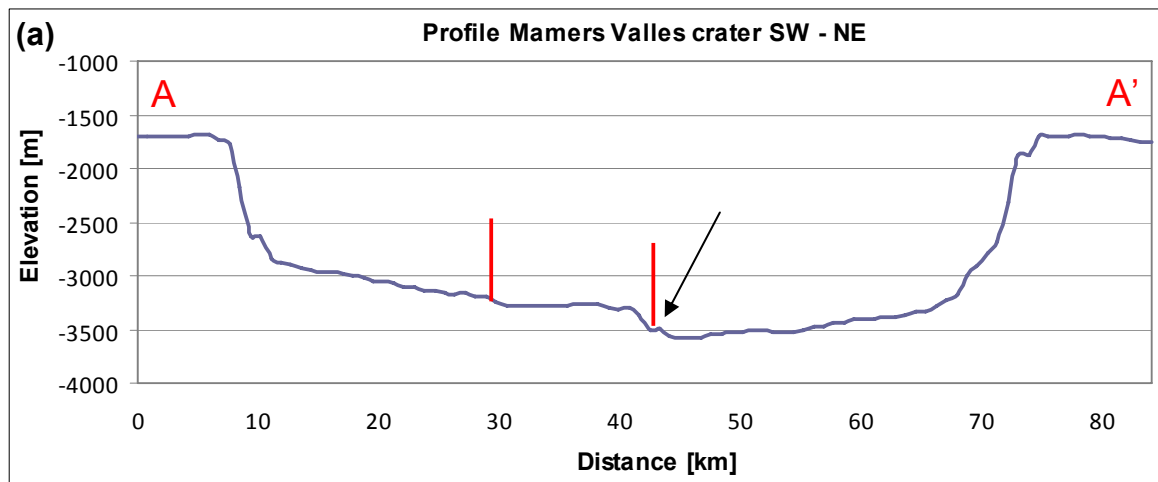


Figure 46: Analysis of the floor topography of the crater shown in Fig. 44 revealing a depression as a potential site for a melt water pond close to the dark patch.

(a) MOLA profile from SW to NE (A – A'). The red marks define the extent of the dark patch. The black arrow marks the location where the dark material would have been deposited in the pond or puddle. **(b)** HRSC colour-coded DTM overlaid on a nadir image (2192_0009). Red line marks the course of the profile from SW to NE (A – A') shown in Fig. a. (see text for discussion)



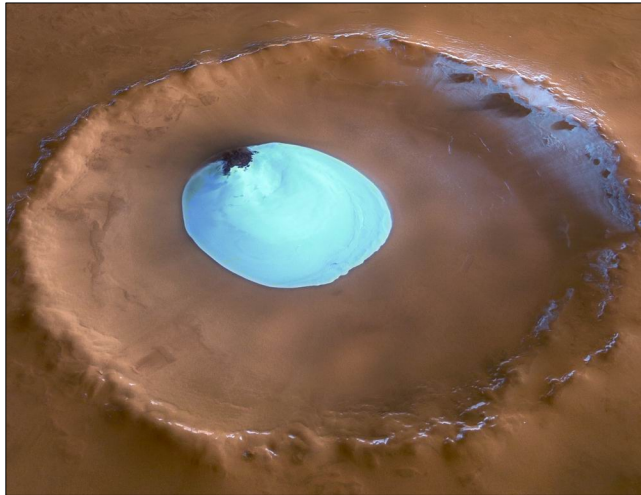


Figure 47: Dark material covered by an ice cap in a crater in Vastitas Borealis (70.5°N, 103.0°E). This example proves the coexistence of ice and dark material on Mars, which might possibly be analogues with the former situation in the crater in Fig. 44, following the scenario in Fig. 45, case Ia and Ib (HRSC perspective view 1343_0000; © ESA/DLR/FUB (G. Neukum)).

During this analysis, it emerged that olivine not only occurs rarely but also appears predominantly in the material of small active-looking fresh dunes and sand sheets (cf. Sect. 5.5.2). Moreover, in the case of Rabe Crater (Noachis Terra, -43.9°S, 34.8°E), olivine was detected in a dark layer exposed in the wall of an intra-crater pit, as shown in Fig. 48. Spectral ratios of dark layer spectra to reference spectra confirm the presence of olivine in this dark layer. As discussed in Sect. 5.2, the dark layers are supposed to be a local source of the dark material inside the craters. This idea is also confirmed by *Fenton (2005b)*, who analyzed the morphology of these layers and found that the dark gullies are probably pathways of sand transport from the pit wall to the interior dunes in Rabe Crater.

Material coming out of the walls might be very fresh, having not been exposed to the atmosphere for a long time. This is in contrast to the pyroxene-rich material that constitutes the intra-crater deposits. It takes at least 2×10^6 years to accumulate massive sand deposits >300 m deep on Mars, a figure deduced from terrestrial analogues by *Breed et al. (1979)* which also applies to the Rabe Crater dune field (dune field volume 77 - 1143 km³ [MCD³, *Hayward et al., 2007b*]; dune field height at least 287 m as measured in the MOLA topography map). During this long dune development, the dark minerals are exposed to the atmosphere and their disintegration and alteration progresses. Because they crystallize at higher temperatures, olivine minerals are less stable at low Martian temperatures and weather earlier to smaller grain sizes than pyroxene minerals, although olivine is more solid than pyroxene [*Matthes, 2001*]. In mineral mixtures, smaller grains are more difficult to detect than coarser grains, as *Poulet et al. (2007)* found when they tested synthetic spectra of different grain sizes and olivine concentrations. Grain size is particularly critical for olivine detection because it strongly affects the 1- μ m band due to the interaction of the shorter wavelength with the particle size [*Poulet et al., 2007*]. Grain size differences of individual olivine and pyroxene particles result in shallower 1- μ m absorption band depths for smaller particles (cf. Sect. 5.3.1). Thus, small olivine minerals are the first to disappear from spectral signature. The occurrence of

olivine in the fresh dark layer and the lack of olivine in the remaining the dune field support the suggestion of relative young and fresh olivine particles, which quickly break down into smaller grain sizes, and pyroxene particles, which are more stable with time. An additional indication for that scenario is the absence of olivine in the other huge dune fields but its occurrence in small unconsolidated dunes, which might be younger than the huge and consolidated ones. Thus, the low prevalence of olivine in the spectra of the dunes might reflect its faster thermal and mechanical erosion under Martian conditions.

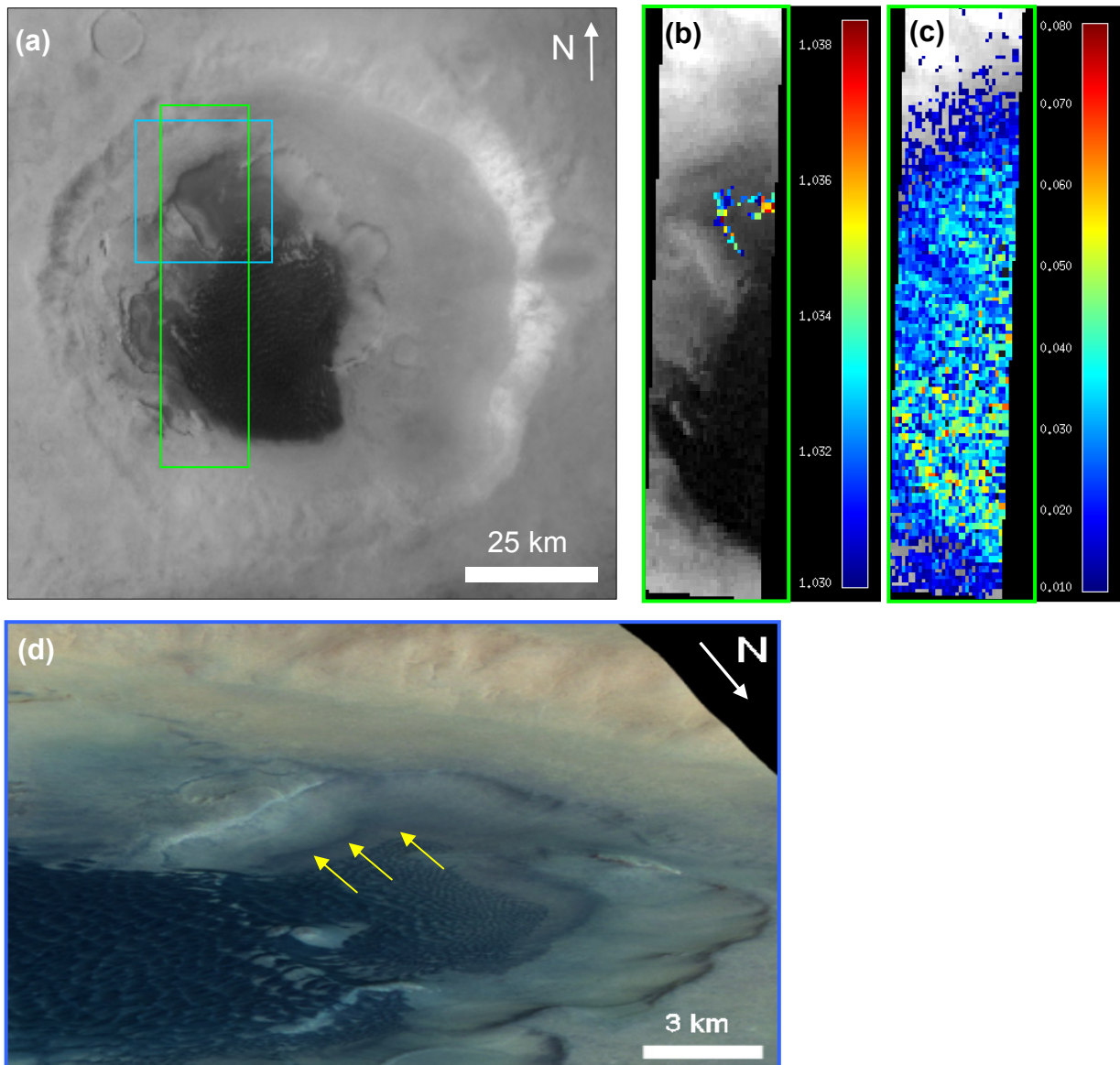


Figure 48: Spectral analysis of a dark layer exposed in an intra-crater pit at Rabe Crater (43.9, 34.8°E). **(a)** Plan view of Rabe Crater showing the footprints in Fig. b, c and d, identifiable by their outline colours (HRSC nadir mosaic of 4280_0000, 4269_0000 and 4258_0000). **(b)** Mapping of olivine inferred from the 1- μm absorption band. **(c)** Mapping of pyroxene inferred from the 2- μm absorption band. **(d)** HRSC perspective view towards the south-west showing the dark olivine-bearing layer in Fig. b (HRSC colour composite 2441_0000).

High-resolution CRISM spectral analyses of the dark layers exposed in crater walls confirm the suggestion that the dark wall material and the dune material are of similar mineralogical composition. Spectra of dark material emanating from a dark layer exposed in the wall of a crater at Terra Sirenum (Fig. 49) exhibit obvious signatures of olivine and pyroxene. Several dark dunes are deposited just down-slope of this crater wall where dark material emerges from the dark layer. Spectral analyses of the dunes reveal an obvious pyroxene content. However, the dune material shows no strong olivine absorptions. This observation is similar to the situation at Rabe Crater mentioned above. The lack of strong olivine signatures in the dunes of this crater could be an additional indication of the disappearance of olivine from dark materials exposed to the surface for a long time due to its faster disintegration to smaller grain sizes. This grain size effect (see above) is the reason why so little olivine has been detected in the dunes. In this scenario, the wall material is of coarser grain than the dune material. This seems reasonable because the grain size of the layered wall material has not yet been reduced, whereas the dune material is already reduced by mechanical splitting to the smaller grain sizes of aeolian sands. Additionally, the dune material is mixed with pyroxene, which complicates the detection of olivine whose absorption band depths are shallower (cf. Sect. 5.3.1). Consequently, the method employed may not accurately identify olivines in mixed dune material if its grain size is in the micrometer range [Poulet *et al.*, 2007] However, the concurrent mafic composition results establish a mineralogical association between the wall and the dune material. Accordingly, the dark layers may be supposed to be a local source of the intra-crater dune material (see also *Tirsch et al.* (2007)).

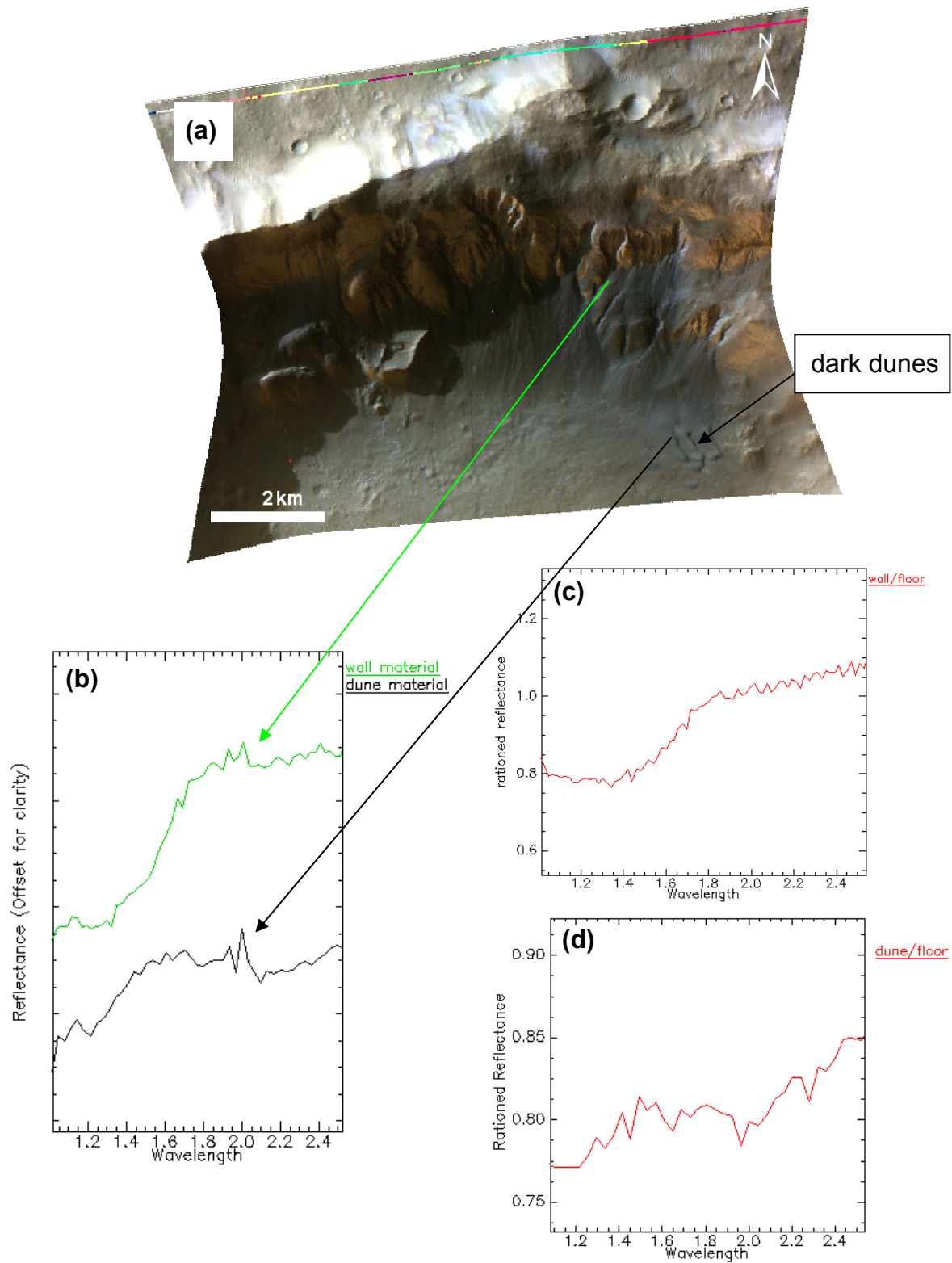


Figure 49: CRISM spectral analysis of dark material emanating from a dark layer exposed in a crater wall. Reflection spectra of dark material emanating from the crater wall show a similar mafic composition as the dune material. **(a)** CRISM observation showing the wall of a crater in Terra Sirenum (39.3°S, 196.0°E). Green and blue arrows marks the locations where the wall and dune spectra of Fig. b were taken (CRISM FRT00003266, colour-composite of bands 13 (1.08 μm), 87 (1.5 μm), and 233 (2.5 μm)). **(b)** Reflection spectra of wall (green curve) and dune material (black curve). The wall material curve exhibits pyroxene as well as strong olivine absorption, whereas the dune material spectrum (black curve) shows a pyroxene signature only. **(c)** CRISM spectral ratio of wall material and crater floor emphasizing the olivine signature of the dark wall material. **(d)** CRISM spectral ratio of dune material and crater floor emphasizing the pyroxene signature of the dark dune material.

A global view of the mineralogy of all dune fields and sand sheets examined is given in Fig. 50. As may be assumed from the local analyses, pyroxene is the dominant mineral in the global view as well. Olivine minerals were detected in 21 localities. In each, olivine exists in association with pyroxene, which is the major component. This is consistent with the results of *Poulet et al.* (2007) who found that olivines on Mars mostly occur in combination with pyroxene. Only seven localities show no obvious mafic spectral signature. Here, the flat and featureless spectral shape indicates the presence of a dust layer on top of the dunes and dune fields. In three localities at higher latitudes, the mineralogical composition of the dark material could not be assessed because layers of water ice covered the surface of the dark material. However, in 59 out of 70 localities where dark material occurs, a mafic composition comprising pyroxene and olivine could be confirmed. This is consistent with the findings of many authors [e.g. *Bandfield*, 2000; *Christensen et al.*, 2000; *Wyatt et al.*, 2001; *Bandfield*, 2002; *Wyatt and McSween Jr.*, 2002; *Christensen et al.*, 2003; *Erard et al.*, 2004; *Bibring et al.*, 2005; *Bibring et al.*, 2006; *Poulet et al.*, 2007]. The results show that the dark material in the depressions analyzed is of the same mineralogical composition overall. Furthermore, its mineralogical composition does not correlate with any geographic or topographic position on Mars in terms of mafic minerals. Thus, it can be supposed that the unoxidized dark materials in Martian craters might have the same origin and did not experience contact to liquid water or other oxidizing agents. See Chapter VI for a detailed discussion of that topic.

The detection of hydrated minerals, however, shows certain clusters in northern Arabia Terra and Meridiani Planum. For instance, the northern margin of Arabia Terra must have experienced a long history of aquatic processes, as evidenced by outflow channels and valley networks such as Mawrth Vallis and Mammers Valles [*Jaumann*, 2003]. Meridiani Planum is assumed to have experienced significant groundwater upwelling and evaporation [*Andrews-Hanna et al.*, 2007b]. The water-related processes in these regions are supposed to have resulted in the formation of various minerals pointing to the former existence of water, such as phyllosilicates, sulphates, and haematite [e.g. *Hynek et al.*, 2002; *Loizeau et al.*, 2007a; *Poulet et al.*, 2008]. Thus, the detection of hydrated minerals in these regions seems to be associated with the geographical location (cf. Sect. 5.6). Because the aquatic processes and the occurrence of chemically unaltered dark material may not cover the same time scale, it is likely that the hydrated spectral signatures detected are associated more with eroded older terrain material than with dark dune material. Alternative effects of a later local alteration of dark material, as discussed above, cannot be ruled out.

The diagram in Fig. 51 presents the statistic of the mineralogical analysis, quoting the detection incidence of each mineral in absolute figures.

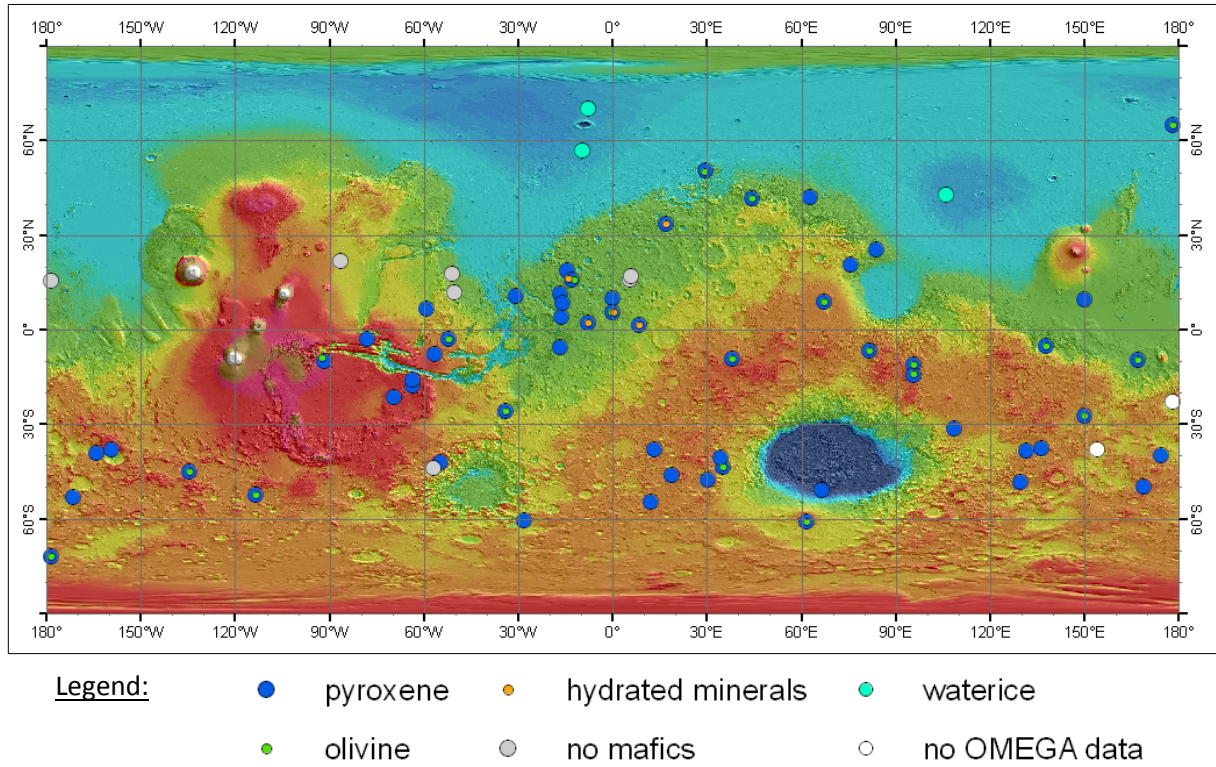


Figure 50: Global consideration of the mineralogical composition of dark intra-crater deposits (background: MOLA topography map).

In general, the homogeneous distribution indicates no correlation between mineralogical composition and geographical location indicating a similarity in material origin. (see text for further discussion)

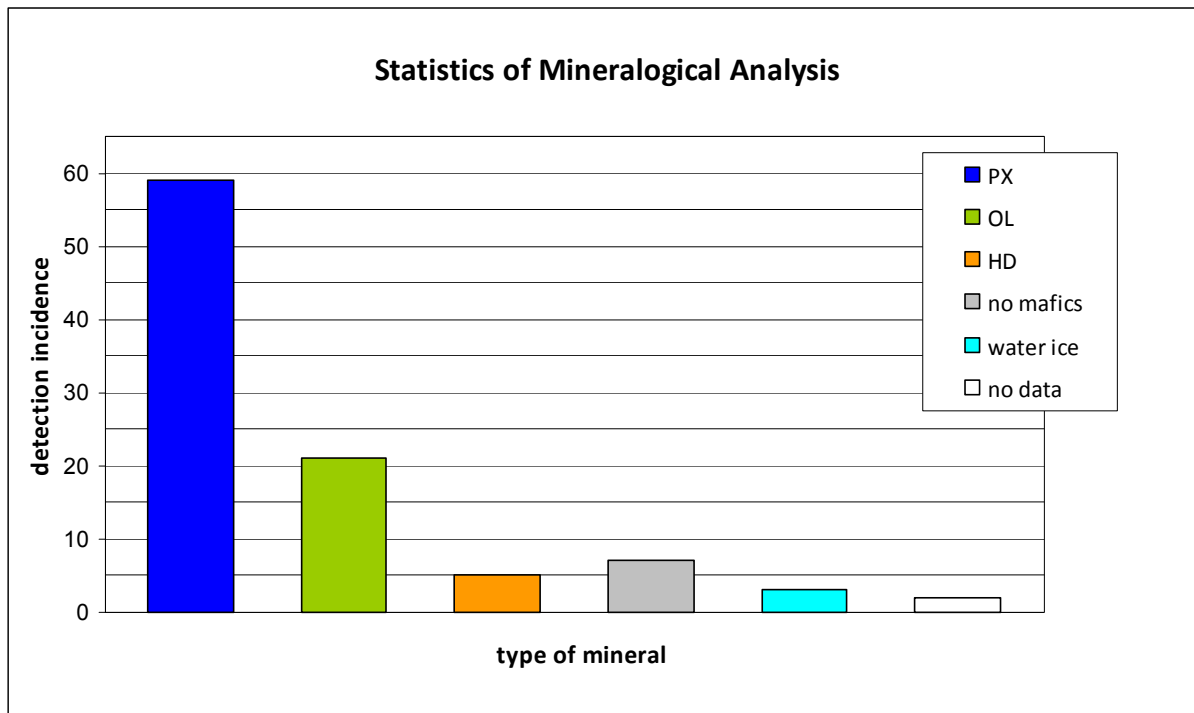


Figure 51: Statistic of the mineralogical analysis.